Research Article

Decellularized peripheral nerve grafts by a modified protocol for repair of rat sciatic nerve injury
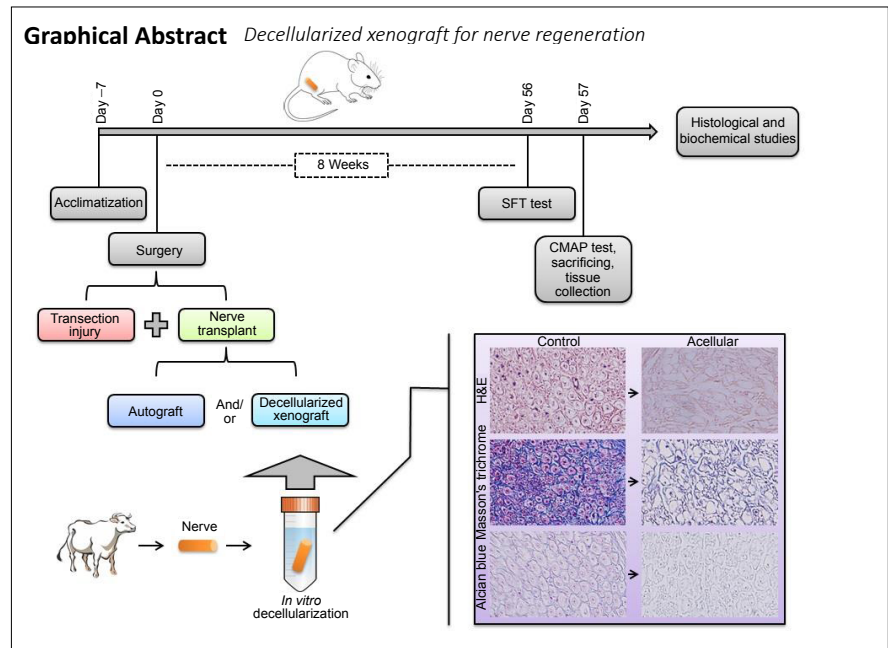
Arash Zaminy[1, *], Sara Sayad-Fathi[1], Farshad Moharrami Kasmaie[2], Zohreh Jahromi[2], Adib Zendedel[3]

Graphical Abstract *Decellularized xenograft for nerve regeneration*

Abstract

Studies have shown that acellular nerve xenografts do not require immunosuppression and use of acellular nerve xenografts for repair of peripheral nerve injury is safe and effective. However, there is currently no widely accepted standard chemical decellularization method. The purpose of this study is to investigate the efficiency of bovine-derived nerves decellularized by the modified Hudson's protocol in the repair of rat sciatic nerve injury. In the modified Hudson's protocol, Triton X-200 was replaced by Triton X-100, and DNase and RNase were used to prepare accelular nerve xenografts. The efficiency of bovine-derived nerves decellularized by the modified Hudson's protocol was tested *in vitro* by hematoxylin & eosin, Alcian blue, Masson's trichrome, and Luxol fast blue staining, immunohistochemistry, and biochemical assays. The decellularization approach excluded cells, myelin, and axons of nerve xenografts, without affecting the organization of nerve xenografts. The decellularized nerve xenograft was used to bridge a 7 mm-long sciatic nerve defect to evaluate its efficiency in the repair of peripheral nerve injury. At 8 weeks after transplantation, sciatic function index in rats subjected to transplantation of acellular nerve xenograft was similar to that in rats undergoing transplantation of nerve allograft. Morphological analysis revealed that there were a large amount of regenerated myelinated axons in acellular nerve xenograft; the number of Schwann cells in the acellular nerve xenograft was similar to that in the nerve allograft. These findings suggest that acellular nerve xenografts prepared by the modified Hudson's protocol can be used for repair of peripheral nerve injury. This study was approved by the Research Ethics Committee, Research and Technology Chancellor of Guilan University of Medical Sciences, Iran (approval No. IR.GUMS.REC.1395.332) on February 11, 2017.

Key Words: acellular scaffold; axonotmesis; bovine; crush injury; detergent; rat; sciatic nerve; xenograft

Chinese Library Classification No. R459.9; R617; R741

Introduction

Following peripheral nerve injury (PNI), Wallerian degeneration occuring in the axon distal stump causes denervation of surrounding body organs (Hall, 2005).

Although in severe injuries, axons are capable of regeneration, but inaccurately targeted reinnervation causes inadequate operative rehabilitation, leading to significant long-lasting impairment (Walsh and Midha, 2009). For long nerve gaps,

[1]Neuroscience Research Center, School of Medicine, Guilan University of Medical Sciences, Rasht, Iran; [2]Student Research Committee, School of Medicine, Guilan University of Medical Sciences, Rasht, Iran; [3]Institute of Neuroanatomy, Faculty of Medicine, Rheinisch-Westfälische Technische Hochschule (RWTH) Aachen University, Aachen, Germany
*Correspondence to: Arash Zaminy, PhD, zaminy_a@gums.ac.ir.
https://orcid.org/0000-0002-2388-481X (Arash Zaminy)

the suturing approach is not desirable, and the present reference surgical method remains to be the autologous nerve grafting. There is a limitation for nerve repair using autograft, as an inadequate number of autologous nerves are accessible for the defective major nerve. This prompts the researchers to look for an alternate method of restoration in broad nerve damages (Siemionow and Sonmez, 2007). The corporal direction of axons has been shown to be a major part of nerve repair (Zilic et al., 2016). The nerve channel should have proper biocompatibility, appropriate biodegradability, adequate mechanical strength, and elasticity. However, thus far no alternatives have been developed as efficiently as the autograft for nerve restoration (Wakimura et al., 2015). One approach for achieving the purpose is via tissue decellularization. This is realized by eliminating immunogenic constituents of the target tissue and retaining the extracellular matrix (ECM) elements and the 3D structure at a subcellular scale. The justification for decellularization is that ECM elements are broadly maintained among species and are also not unfavorably immunogenic (Zilic et al., 2016).

Since autograft and allograft usage and availability have some limitations (Anderson, 2006), the use of xenogeneic nerves augments the source of grafts broadly, therefore it has an encouraging perspective for the clinical therapy. Currently, there are few reports about the application of acellular nerve xenografts (ANX) and their biocompatibility to treating nerve injury (Jia et al., 2012).

The application of xenogeneic tissue suggests a fascinating substitute method for human tissue. Some animal organs are structurally similar to human organs, and they can be used as an interesting alternative to transplant in some particular situations (Zilic et al., 2015). Bovine peripheral nerves are composed of perineurium, epineurium, endoneurial microstructure, and comparable ECM element and structure (Shellswell et al., 1979). Therefore, we hypothesized that bovine peripheral nerves, as an alterative to autograft nerves, can be used for a proper grade of corporal direction and rehabilitation assistance. Several approaches have been recorded for making acellular nerve grafts from donor nerve tissue (Moore et al., 2011). The frequently utilized methods involve several enzymatic, chemical, and physical handlings (Zilic et al., 2016). Chemical processing involves detergents (zwitterion, non-ionic, and ionic), treating with alkaline and acid, hyper and hypotonic solvent and chelator, including ethylenediaminetetraacetic acid (EDTA). These processes are utilized to solubilize both nuclear cellular membranes and cytoplasmic proteins (Crapo et al., 2011). However, an optimized method does not exist, and advanced systems are being studied to prepare tissue-engineered grafts (Sridharan et al., 2015; Geuna et al., 2016). Therefore, the purpose of the present study was to create an efficient method to decellularize peripheral nerves.

Materials and Methods

The experimental procedure consisted of two stages: In stage I, bovine nerve segments were harvested and nerve decellularization was created; in stage II, the decellularized nerves were implanted in Wistar rats to repair sciatic nerve defects.

Ethical consideration
The present study was approved by the Research Ethics Committee, Research and Technology Chancellor of Guilan University of Medical Sciences (IR.GUMS.REC.1395.332) on February 11, 2017.

The animals were maintained in a steady light and dark cycle of 12 hours with *ad libitum* access to food and water. The moisture and temperature were kept consistent at 60% and 22°C, respectively. All efforts were made to reduce pain and distress.

Stage I
Nerve isolation and decellularization process
Bovine nerve samples were obtained from a local abattoir (Lakan, Rasht, Iran), within 6 hours of slaughtering. The brachial plexus nerves were removed from the forelimb of the bovine (n = 3, male, 12 months old). We selected bovine brachial plexus nerves the diameter of which matched with that of rat sciatic nerves. All selected nerves were cut into segments (15–20 mm in length). Nerve segments were decellularized, using a modification of the protocol of Hudson et al. (2004a). All nerve samples were submerged in deionized distilled water (ddH$_2$O) for 12 hours and further treated with 125 mM sulfobetaine-10 (SB-10) solution (Abcam, Cambridge, MA, USA; Cat# 146363; CAS: 15163-36-7) for 12 hours. Following a wash with ddH$_2$O for 15 minutes, the nerves were exposed to 0.6 mM sulfobetaine-16 (Abcam; Cat# ab142103; CAS: 2281-11-0)/0.14% Triton X-100 solution (Sigma-Aldrich, St. Louis, MO, USA, 93443; CAS:9002-93-1) for 12 hours. After a wash with ddH$_2$O for 15 minutes, the nerves were subjected to SB-10 staining for 7 hours, rinsed once, and washed in the sulfobetaine-16 (SB-16)/Triton X-100 solution for 12 hours. Then all nerve samples were rinsed with ddH$_2$O for 15 minutes. Next, the washing solvent was replaced by DNAse/RNase solution, containing 1 U/mL RNase (Cat# R6513; Sigma-Aldrich), 50 U/mL DNAse (Cat# 11284932001; Sigma-Aldrich), 50 mM Tris at pH 7.5, and 10 mM MgCl$_2$ for 6 hours (the solution was changed after 3 hours). Finally, all nerve samples were washed with ddH$_2$O for 15 minutes, subsequently stored in PBS containing 100 mg/mL streptomycin and 100 U/mL penicillin (Gibco, Fisher Scientific, UK), and kept at 4°C for at least 48 hours before use. All processing stages were conducted on a shaker at ambient temperature.

Biological evaluation of acellular nerves
To verify the successful decellularization of nerves, the segments were dyed with Gill's hematoxylin and eosin for general evaluation, Alcian blue for sulfated glycosaminoglycans (sGAG), Masson's trichrome for collagen fibers, and Luxol Fast Blue (LFB) for myelin. A light microscope was used to take pictures (BX51, Olympus,Tokyo, Japan).

To evaluate decellularization procedure, the samples were also stained with 4′,6-diamidino-2-phenylindole (DAPI) for the presence of nuclear material remnants, rabbit anti-neurofilament 200 (NF-200) (Cat# ab8135; 1:100; Abcam) for axons, rabbit anti-S-100 (Cat# ab868; 1:100; Abcam) for Schwann cells and rabbit anti-laminin (Cat# ab11575; 1:200; Abcam) and rabbit anti-collagen IV (Cat# ab6586; 1:100; Abcam) at 4°C overnight. The secondary antibodies were horseradish peroxidase (HRP) (Cat# ab6721; 1:1000; Abcam) or fluorescein isothiocyanate (FITC) (Cat# ab6717; 1:1000; Abcam) goat anti-rabbit antibody for 2 hours at room tempreture. The 3,3-diaminobenzidine substrate (DAB) (SIGMAFAST™ DAB with Metal Enhancer, Sigma; Cat# D0426) was used to visualize the positive spots. For immunohistochemistry quantification, three samples of each group, and five sections of each sample at equal intervals, were selected. All positive areas, in five microscopic high-power fields (400×) randomly selected in each section, were analyzed and averaged.

For further ultrastructural analysis, scanning electron microscopy (SEM) (MIRA3 FE-SEM Tescan, Brno, Czech Republic) with a lens detector under 5 kV acceleration voltages, was used to examine the samples at calibrated magnifications.

DNA quantification
DNA was quantified to assess the remaining DNA in bovine peripheral nerves. The amount of DNA was compared between fresh and decellularized tissues. DNA was extracted using the DNA extraction kit (GeNet Bio, Daejeon, Korea).

Research Article

A nanodrop (Labtech, Heathfield, Sussex, UK) was used to spectrophotometrically assess the concentration of DNA at 260 nm. The latest concentration was applied to compute the DNA weight/tissue weight (ng/mg).

Cytotoxicity assay of acellular nerve

In order to assess the level of residual detergents in acellular nerves, a cytotoxicity assay was performed. Rat adipose-derived stem cells (ADSCs) were used in this assay (Kashani et al., 2009). Primary ADSCs were isolated from the scrotal fat pad of rats of the same age and weight. Intact bovine nerves that were washed and decellularized bovine nerves that were not washed were used to assess the efficiency of washes during the process of decellularization. The nerve samples of the same size (~2 mm^2) were put into the 96-well tissue culture plates. ADSCs at a density of 10×10^3 cells per well were seeded and stored at 37°C in 5% CO_2 (v/v) for 48 hours. The impact of samples on cell increase (viability/cytotoxicity) was initially determined through assessing the dye absorbance of 3-(4.5-dimethylthiazol-2-yl)-2,5-diphenyl tetrazolium bromide (MTT) by the cells. Three wells were analyzed for each condition by an ELISA reader (800 TS, BioTek, Winooski, VT, USA).

Hydroxyproline assay

Hydroxyproline (HYP) assay was conducted to assess the full residual collagen, persisting in bovine peripheral nerves, after decellularization. The HYP assay kit (KIAZIST, Hamedan, Iran) was used to assess the total protein content in nerve samples based on the manufacturer's instruction.

Stage II
Surgery

Thirty-two young and adult male Wistar rats (6–8 week olds), initially weighing 250–300 g, with a mature skeleton, clinically and functionally healthy were used. All animals (Pasteur Institute of Iran, Tehran, Iran) were categorized into four groups (*n* = 8): sham, negative control (nerve defect; ND), nerve autograft (NA), and acellular nerve xenograft (ANX). First, the animals were evaluated before the injury, to make sure that each sciatic functional index has regular functioning. Each rat was sedated by an intraperitoneal injectin of xylazine (10 mg/kg; Webster Veterinary Supply, Sterling, MA, USA) and ketamine (100 mg/kg; Webster Veterinary Supply) to reduce the pain and suffering experienced by laboratory animals.

After the blunt removal of muscles, an incision was made in the posterior aspect of the left thigh, and the sciatic nerve was uncovered. In the NA group, a 7 mm long nerve segment was dissected, reversed, and then microsurgically sutured back with a 10.0-gauge suture. In the ANX group, a 7 mm long nerve segment was dissected and substituted by a decellularized bovine nerve segment of the same length. In the ND group, a 7 mm long nerve segment was removed and no graft was used. In the sham group, after incision creation, nerve sectioning was not performed. Once the action was completed, rats were supervised while recovery from sedation, warmed using heat lamps, and allowed to take drink and food *ad libitum*.

Calculation of sciatic functional index

At 1, 2, 4, 6 and 8 weeks after surgery, sciatic nerve function-related parameters of both hind limbs were collected, and SFI was computed based on the formula outlined in a previous study by Bain et al. (1989).

Electrophysiological evaluation

Electrophysiological study was carried out on animals before slaughter. A bipolar stimulating electrode (1000 mA) was positioned at the proximal area of grafts, and a second electrode was placed on the gastrocnemius muscle (frequency of 0.2 Hz). The elicited action potential, in response to the impulse, was reported (eWAVE8D, science beam, Teharn, Iran), and then the latency was calculated.

Determination of recovery rate of rat gastrocnemius wet weight

Eight weeks after surgery, rat gastrocnemius muscles were taken, and their wet weight was recorded. The wet weight recovery rate (%) was calculated using the formula as follows: (muscle wet weight on the surgical site/muscle wet weight on the non-surgical site) × 100.

Histological evaluation

The grafts that demonstrate all experimental requirements were collected 8 weeks after surgery. The sciatic nerve was then cross-sectioned, 5 mm below and above the graft. Paraffin sections of sciatic nerve tissue, 5 μm thick, were then dyed with hematoxylin and eosin for general evaluiation and with LFB for myelin.

In addition, immunostaining was performed with anti-NF-200 and anti-S100 primary antibodies at 4°C overnight. DAB substrate and HRP-conjugated secondary antibody were used to visualize the nerve fibers and Schwann cells. The dyed sections were envisioned on an Olympus BX51 (Olympus, Tokyo, Japan) inverted microscope. For quantification, five sections of each animal were chosen at equal intervals. All positive spots in five randomly selected microscopic high-power fields (400×) for each section were examined and the mean of positive spots per section was calculated.

Statistical analysis

GraphPad Prism v7.0 software (GraphPad Software Inc., San Diego, CA, USA) was used to perform statistical analysis. The analysis of variance with Tukey's *post hoc* test was performed by one-way ANOVA for comparison among multiple groups. The unpaired *t*-test was used for comparison between two groups. $P \leq 0.05$ was considered statistically significant. Graphical and numerical data are reported as the mean ± standard deviation (SD).

Results
Stage I
Decellularization results

For cell removal, three different detergents were used. Histological staining was performed once the process of decellularization was completed. Improved elimination of cellular content by detergent was histologically confirmed (**Figure 1**). The hematoxylin and eosin (H&E; **Figure 1A**) and Mason's trichrome (**Figure 1C**) staining of the native tissue demonstrated the existence of a tight mesh of parallel collagen fibers with the appearance of cells across the samples. A significant level of cellular eliminations was shown by detergent treatment, but also led to the minimal interruption of fibers. In the treated group, collagen fibers demonstrated no considerable morphological alterations, in comparison with native nerves (**Figure 1B** and **D**). Alcian blue staining (**Figure 1E** and **F**) was used to localize sGAG. The Alcian blue staining showed reservation of connective tissue and nerve fascicles, as also sGAG. Another important part of a nerve is myelin sheath. LFB staining was performed to assess myelin removal (**Figure 1G** and **H**). The LFB staining revealed that myelin sheath was efficiently cleaned in almost all nerve samples. The anti-NF-200 staining protocol was performed to verify the presence of axons in the samples. The control nerves demonstrated the presence of consistent and well-maintained axons (**Figue 3A**); while nerves in all samples were negative for Triton X-100, SB-10, and SB-16 staining (**Figure 3B** and **Table 2**). DAPI nuclear staining was performed to detect nuclear material remnants (**Figure 1I**). Most samples were negative, but some sections showed a negligible DAPI positivity, indicating that cell content was removed efficiently

(**Figure 1J**). In addition, tissue segments were dyed for S-100 protein to determine the elimination of cellular constituents by decellularization (**Figure 4A** and **B**). After decellularization, Schwann cell debrises were observed in the tissue, using stain for S-100. No noticeable stain was observed in sections, where Schwann cells were eliminated by detergents (**Figure 4B** and **Table 2**). In consideration of the importance of ECM, collagen IV and laminin, two important components of ECM, were evaluated with anti-collagen IV (**Figure 5A**) and anti-laminin (**Figure 5B**) antibodies. Immunohistochemical staining demonstrated that these proteins were preserved well (**Figure 5C** and **D**). In all processed samples, the general framework of the axially arrayed collagen fibers was kept intact.

DNA content
DNA, 0.62 ± 0.49 ng/mg, was found in the native nerve tissue (**Table 1**). After detergent treatment, DNA content was significantly reduced to 0.04 ± 0.042 ng/mg ($P < 0.05$), which is equal to 93.5% reduction.

Collagen content
The collagen content is corresponding directly to the HYP content. HYP, 2.71 ± 0.14 mg/mL, was found in the native nerve (**Table 1**). The decellularized group had an HYP content of 2.45±0.11 mg/mL, which was about 9.5% lower than that in the native tissue. As the results show, the decellularization protocol had no significant effect on the content of collagen ($P > 0.05$).

Contact toxicity
Detergents can occasionally be maintained in decellularized samples, which can be cytotoxic. Thus, a cytotoxicity assay was carried out. ADSCs were chosen, as they are easy to access and use. ADCSs were noted microscopically and those that multiply and expand normally were identified. MTT assay showed no sign of cell toxicity and no considerable difference was identified between the native and decellularized classes (**Figure 6**).

Ultrastructure of decellularized nerves
The scanning electron microscopy images of the decellularized nerves revealed that the communicating structure of the nerve ECM was preserved well, while axon and Schwann cell contents were eliminated substantially (**Figure 7**).

Stage II
Histological evaluation
In the ANX group, eight weeks after surgery, H&E staining (**Figure 2A** and **B**) demonstrated well integration of the nerve and grafts, and a tissue bridge formation between the caudal and rostral ends of the sciatic nerve. The data from H&E staining also demonstrated significant host cell penetration in the scaffolds. In ANX sections, several vessels showed revascularization and good integration of xenografts with host tissue. The LFB staining results revealed the remyelination of the budding axons in the scaffolds of decellularized nerve (**Figure 2C** and **D**). Following graft decellularization, the impact of grafts on nerve fiber budding was determined by NF-200 staining (**Figure 3C** and **D**). NF-200 immunohistochemical staining showed a broad axonal expansion into the decellularized graft, at 8 weeks post-implantation. The number of NF-200 positive nerve fibers was increased in the NA group, compared to the ANX group (**Table 2**). However, the difference was not statistically significant. The S100 immunohistochemistry staining showed that Schwann cells were available in all subjects of decellularized grafts (**Figure 4C** and **D**). The quantification of Schwann cells demonstrated no noticeable difference between the NA and ANX groups (**Table 2**). In the ANX group, some Schwann cells integrated linearly in the scaffold, along with the long axis of the graft. DAPI staining (**Figure 2E** and **F**) showed many positive cells in the grafts. In

the decellularized nerve, the number of cells was significantly higher than that in the autograft.

Motor function
To evaluate motor function recovery, walking analysis was employed to create an SFI estimate for every animal at equal intervals up to the 8th week (**Figure 8**). As shown in **Figure 8**, the functional recovery of the xenograft was slightly, but not significantly ($P > 0.05$), better thn that of the autograft. The average SFI at 8 weeks was −2.70 ± 1.76, −43.1 ± 12.42, −40.22 ± 10.57 and −65.15 ± 7.74 for the sham, NA, ANX, and ND groups, respectively. The ND group demonstrated a far lower recovery, compared with the ANX and NA groups. In the sham group, the surgical process without nerve cross-section was not affected by the surgery and motor function restored in all rats.

Electrophysiological results
At 8 weeks after surgery, compound muscle action potentials (CMAP) were determined in five rats of each group. No noticeable difference was found in the latency among the groups (**Table 2**).

Muscle wet weight
At 8 weeks after surgery, the recovery rate of the wet weight of the gastrocnemius muscle was significantly higher in the NA and ANX groups than that in the sham and ND groups ($P < 0.05$), but there was no significant difference between NA and ANX groups ($P > 0.05$; **Table 2**).

Discussion
The objective of the present study was to establish a procedure to decellularize the peripheral nerve, with minimum impact on tissue characteristics. The principal results of the study showed a mixture of zwitterionic and non-ionic detergents, and nuclease enzymes exhibited effective property in cell removal of bovine nerve tissue though maintaining the associated endoneurial frame and important
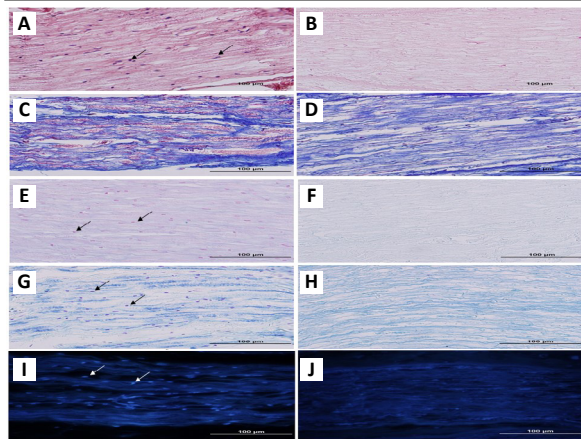
Figure 1 | Histological sections from the native and decellularized bovine nerves.
Bovine peripheral nerves were stained for collagen, sulfated glycosaminoglycans, myelin, and nucleus materials. Sections of native (left column) and decellularized nerve (right column) were stained, using hematoxylin & eosin (A, B). The Masson's trichrome staining (C, D) demonstrates the presence of a tight network of parallel collagen fibers (the pink color indicates the myelin sheaths). The detergent treatment showed a high degree of cellular removal. Alcian blue staining (E, F) demonstrated retention of nerve fascicles and connective tissue, as well as sulfated glycosaminoglycans. Luxol fast blue (G, H) staining revealed that almost all the nerve samples were cleaned from myelin sheaths efficiently. Most samples were 4′,6-diamidino-2-phenylindole (DAPI)-negative (I, J), but in some sections a negligible DAPI positivity was observed, indicating that cell content was removed efficiently. Arrows indicate the nuclei. Scale bars: 100 μm.
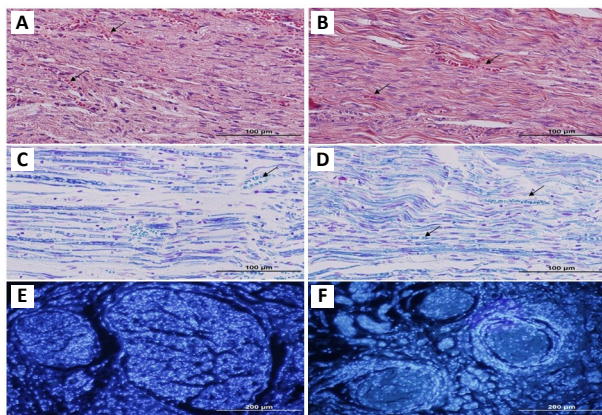

Figure 2 | Histological sections of nerve graft from the NA and ANX groups.
Eight weeks after graft implantation, grafts were collected and stained for histomorphometric evaluations. Hematoxylin & eosin staining revealed well integrity and revascularization of the graft (A, B). In grafts, Luxol fast blue staining (C, D) demonstrated the presence of myelin sheaths, especially in ANX. 4′,6-Diamidino-2-phenylindole staining (E, F) showed many positive cells in grafts. In the decellularized nerve, the number of positive cells is observed more obviously, compared with the autograft. Arrows show vessels. (left column: NA, right column: ANX). Scale bars: 100 μm in A–D, 200 μm in E and F. ANX: Acellular nerve xenografts; NA: nerve autograft.
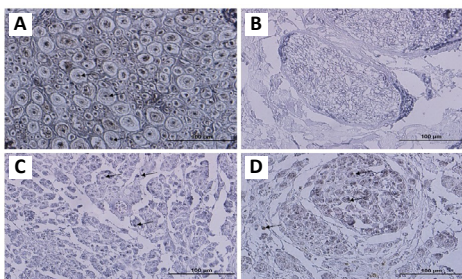

Figure 3 | Immunohistochemistry staining of anti-NF-200.
Sections of native (A) and decellularized nerve (B) were stained by the anti-NF-200 antibody. Immunohistochemistry showed that nerve fibers were removed by the decellularization process (B). After 8 weeks, staining of NA (C) and ANX (D) grafts showed that many NF-200 positive myelinated axons were observed throughout the grafts, and in the xenografts as well. Arrows indicate the axons. Scale bars: 100 μm. ANX: Acellular nerve xenograft; NA: nerve autograft; NF-200: neurofilament 200.
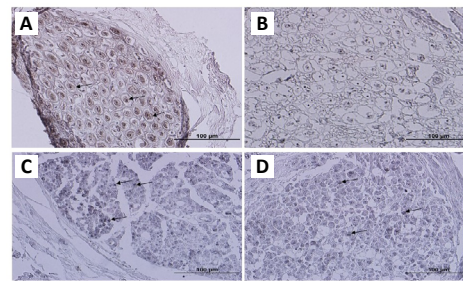
Figure 4 | Immunohistochemistry staining of anti-S-100 of the native and decellularized bovine nerves.
Immunostaining of native (A) and decellularized nerve sections (B) by anti-S-100 antibody showed no visible stain in sections, where Schwann cells were eliminated by detergents. After 8 weeks, staining of NA(C) and ANX(D) grafts showed that many S-100 positive spots are found in the auto and xenografts. Arrows indicate the axons. Scale bars: 100 μm. ANX: Acellular nerve xenografts; NA: nerve autograft.
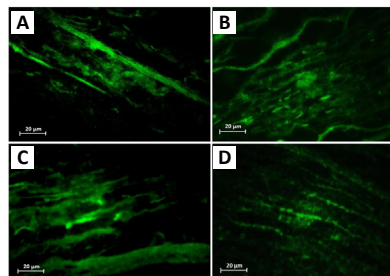

Figure 5 | Effect of decellularization process on the extracellular matrix structure of the native and decellularized bovine nerves.
Bovine nerves were stained by immunofluorescence antibodies for collagen IV and laminin before (A, B) and after decellularization (C, D). Staining revealed retention of laminin and collagen within grafts. Scale bars: 20 μm.
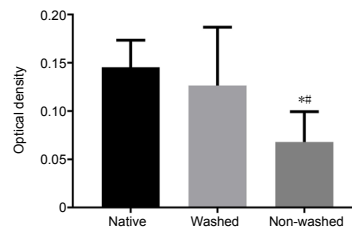

Figure 6 | Cytotoxicity assay of the native and decellularized bovine nerves.
The effect of decellularized bovine nerves on primary rat adipose-derived stem cells was evaluated after 48 hours by MTT assay. Decellularized nerves after washing did not show any significant adverse effects ($P > 0.05$). Due to residual detergents, non-washed decellularized nerves had a negative effect on cell viability. The experiment was repeated at least three times. The optical densities were compared among the three groups by 4′,6-diamidino-2-phenylindole ($n = 12$). *$P < 0.05$, vs. native group; #$P < 0.05$, vs. washed group. Data are shown as the mean ± SD.
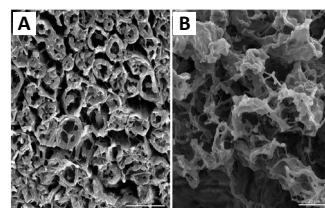
Figure 7 | Scanning electron micrographs of bovine nerve samples before (A), after (B) decellularization.
The communicating structure (stars) is preserved, and cellular contents are eliminated substantially. Scale bars: 20 μm.
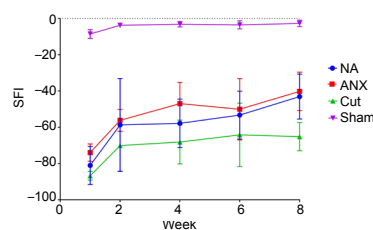
Figure 8 | Walking analysis of rats.
SFI measured in the four experimental groups at 1, 2, 4, 6 and 8 weeks after surgery, and the SFI value was calculated. In the 8th week, the results showed no significant difference between NA and ANX groups ($P > 0.05$). Data are shown as the mean ± SD ($n = 7$). ANX: Acellular nerve xenograft; NA: nerve autograft; ND: negative control; SFI: sciatic functional index.

ECM constituents. The present study also demonstrated no cytotoxicity of acellular nerve and the retention of 3D structure. The nerve graft and encompassing tissues had no acute, sub-acute, or chronic rejection. No sign of graft distention and necrosis was found. Histological staining revealed no severe mononuclear cell infiltration in the graft, suggesting that such process prevented against adverse immune reactions.

ECM was employed for scaffolding usually from a xenogeneic origin, for the substitutions or regeneration of several tissues. Even though ECM has been reported to be acceptable for scaffolding in tissue repair, its preparation procedure can drastically change the host remodeling reaction (Badylak, 2004).

Our study demonstrated that the nerve frame with the retention of the basal membrane was preserved, following the established decellularization procedure.

Masson's trichrome and H&E staining displayed the collagen fibers of the processed nerves, like the control nerves, suggesting that the process of decellularization had no impact on ECM. Wallis et al. (2012) reported the importance of retaining the virtue of the ECM to reach proper recellularization. For more evaluation of ECM, we performed immunohistochemistry using anti-collagen 4 and laminin antibodies. Our staining results showed that these two components were almost preserved well during the process of decellularization. In the mammalian ECM, the most abundant protein is collagen. Collagen represents more than 90% of the dry mass of the ECM in majority of organs and tissues (Van Der Rest and Garrone, 1991). In addition, laminin is a complicated adhesion protein present in the ECM, specifically within the basal membrane (Schwarzbauer, 1999). This protein is the most and first critical ECM factor in tissue differentiation and cell processing, and critical for organizing tissue development (Badylak, 2004).

A benefit of using the ECM in its original condition as a base for cell differentiation and development is the proportional availability of all the involved growth factors (and their inhibitors), existing in an environment and probably much significantly, in their original 3D ultraframe. The ECM offers these factors effectively to cell surface receptors, safeguards the growth factors from deterioration, and modifies their organization (Entwistle et al., 1995; Kagami et al., 1998; Bonewald, 1999). Considering the ECM as a base for *in vivo* and *in vitro* cell development, it is logical to regard the ECM as a transient (i.e. degradable) controlled free medium, for naturally occurred growth factors. Noticeably, all techniques of cell removal of tissue would negatively influence the ECM constituents and create in certain extent, a disruption of ultrastructure. Decreasing, rather than preventing the undesired impacts is the real purpose of decellularization. Physical, chemical and enzymatic agents can be applied. The benefit of physical techniques of decellularization, such as freezing and thawing, is the associated consistent equivalent effect on the entire tissue (Keane et al., 2012). Thermal decellularization is one of the techniques for producing acellular nerve grafts, a process in which the tissue is subjected to repeated freeze-thaw phases. This procedure cannot remove the residues of the destructed cells, therefore, the cell remnants can cause unwanted immunologic or biological effects (Zalewski and Gulati, 1982; Gulati and Cole, 1994). In addition, the structural proteins and basal laminae will be fractured (e.g., collagen, fibronectin, and laminin). Then, through the first days after grafting, Schwann cells and macrophages infiltrate the tubes to clear the cellular residue. This cellular infiltration is thought to slow the process of regeneration and further damage the basal laminae (Osawa et al., 1990; Danielsen et al., 1995).

Thus, it was reasonable to choose enzymatic or chemical treatment to clean the base from the cellular residues. As the enzymatic factors result in less consistent removal and cause noticeable alterations in the ECM arrangement (Gilbert et al., 2006), therefore, chemical agents were applied as a substitute for the clearance and decellularization stage. Among them, normally non-ionic, ionic, or zwitterionic detergents are utilized. There are two common protocols, used frequently by researchers for decellularization and introduced by Snodell et al., (1998) and Hudson et al. (2004a). The Snodell protocol utilizes sodium deoxycholate and Triton X-100, while the Hudson procedure employs SB-16 SB-10, and Triton X-200. Individual comparison of these detergents shows that sodium deoxycholate and Triton X-100 create more skeletal harm to nerve tissue, compared with SB-10, Triton X-200, or SB-16. The Snodell procedure produced more harm to the basal laminae and general morphology, compared with the Hudson technique (Hudson et al., 2004a).

Even with the inclusion of Schwann cells, studies have shown that the Snodell protocol cannot meet the reconstruction percentage found in autografts (Frerichs et al., 2002). It has been hypothesized that the improper retention of the ECM frame in these detergent-processed decellularised graft, is a determinant for failing. Greater retention of original ECM and equal degree of decellularization have been shown, while using milder detergents, in comparison with the former chemical treatment methods (Hudson et al., 2004a). The Hudson's protocol showed considerable positive outcomes among decellularization protocols. However, Triton X-200 is not available anymore on the market (Philips et al., 2018) and also many investigations reported adverse impacts of ionic detergents in ECM ultraframe (Faulk et al., 2014; Xu et al., 2014; Wu et al., 2015; Philips et al., 2018), such as decreased elastin, collagen, laminin, growth factor and sGAG content (Brown et al., 2011; Ren et al., 2013; Faulk et al., 2014). Changes in the skeletal arrangement of ECM upon decellularization can influence function, cell attachment and differentiation; decreased practicality and poor cellular health have been assigned to matrix changes caused by sodium dodecyl sulfate (SDS) and sodium deoxycholate decellularization (Ren et al., 2013; Syed et al., 2014). Whereas, non-ionic (e.g., Triton X-100) detergents are efficient for cell dissection from thin tissues, causing less deterioration of ultraframe and less glycosaminoglycan withdrawal (Velardi et al., 2006), compared to ionic detergents (Faulk et al., 2014). Some zwitterionic detergents, such as SB-16 and SB-10 have demonstrated higher ECM retention and enhanced cell elimination with mild disruption of ultrastructure in thin tissue (Hudson et al., 2004a). Therefore, in the present study, we decided to use Triton X-100, a milder detergent, with Zwitterionic detergents instead of Triton X-200. For more effective decelluraziation, in combination with these detergents, DNase and RNase enzymes were also added in the decellularization protocol to enhance the chemicals' properties. Biochemical, immunohistochemical and histological characterization of the acellular nerve were performed to assess whether the tissue preserved the original histoarchitecture, and maintained the principal ECM constituents. Preservation of original connective tissues and nerve fascicles, in addition to sGAG and collagen, has been shown with histological staining. About a 10% decrease in whole collagen content, was shown in an HYP assay, in comparison to the original nerve, however, it was not noticeable. Fragmented and whole DNA can show an inflammatory reaction, which can result in graft rejection *in vivo*. Less than 50 ng double-stranded DNA per mg ECM dry mass was recommended by Crapo et al. (2011) for a decellularized graft, in addition to no apparent nuclear substance in tissue segments (Crapo et al., 2011), which can be assessed by H&E or DAPI staining. In the present study, DAPI and H&E staining demonstrated a lack of apparent

Research Article

cells from tissue segments and 0.04 ng/mg of DNA, a 93.5% DNA reduction when compared with the fresh tissue. The decellularization procedure cannot remove total DNA from the tissue, even after the most stringent treatment techniques. Trace levels of residual DNA can be found in most available biological scaffolds in the market (Keane et al., 2012). In addition, DAPI staining revealed that decellularized nerves were repopulated by cells after implantation, so that cell number was even more than autografts, which can be Schwann, macrophages and stem/progenitor cells (Costa et al., 2017). A probable reason for the elevated amount of cells in the decellularized grafts, in comparison with the fresh autografts, is that the lack of myelin and the open basal lamina tubes allowed a higher amount of cells to attack and stay within the decellularized grafts. As the cells that entered produce growth factors, this may be useful (Hudson et al., 2004b). Samples also have undergone a histological analysis of nerve reconstruction. Most of the myelinated axons can be well characterized, using conventional staining and immunohistochemistry, and due to dying with LFB and anti-NF-200, myelin sheaths were abruptly specified. These preliminary results proved that this model did not stimulate any adverse impact, by using small sample size, and xenogeneic acellular nerves could provide an appropriate microenvironment for axon myelination and elongation, and nerve reconstruction occurred effectively.

At 8 weeks after surgery, motor function evaluation revealed that the sciatic nerve function had recovered in xenograft and autograft; determination of histologic and electrophysiological restoration also proposed no noticeable distinction among the groups (NA *vs.* ANX). These data optimistically show that through detergent washing, a great functional nerve graft that is as efficient as autograft could be reached from a xenograft.

A completely decellularized and aseptic graft can be obtained using the novel procedure of decellularization and in an acceptable process period. The present study still has some restrictions. Due to the inaccessibility of Triton X-200, we could not compare with the protocol of Hudson et al., and the real difference of our modified decellularization practice remains unrevealed. Also, using a larger sample size, longer gaps and longer observation time is necessary to validate the neuroregenerative efficiency of the newly developed ANX.

References

Anderson M (2006) Xenotransplantation: a bioethical evaluation. J Med Ethics 32:205-208.
Badylak SF (2004) Xenogeneic extracellular matrix as a scaffold for tissue reconstruction. Transpl Immunol 12(3-4):367-377.
Bain JR, Mackinnon SE, Hunter DA (1989) Functional evaluation of complete sciatic, peroneal, and posterior tibial nerve lesions in the rat. Plast Reconstr Surg 83:129-138.
Bonewald LF (1999) Regulation and regulatory activities of transforming growth factor beta. Crit Rev Eukaryot Gene Expr 9:33-44.
Brown BN, Freund JM, Han L, Rubin JP, Reing JE, Jeffries EM, Wolf MT, Tottey S, Barnes CA, Ratner BD, Badylak SF (2011) Comparison of three methods for the derivation of a biologic scaffold composed of adipose tissue extracellular matrix. Tissue Eng Part C Methods 17:411-421.
Costa A, Naranjo JD, Londono R, Badylak SF (2017) Biologic scaffolds. Cold Spring Harb Perspect Med 7:a025676.
Crapo PM, Gilbert TW, Badylak SF (2011) An overview of tissue and whole organ decellularization processes. Biomaterials 32:3233-3243.
Danielsen N, Kerns JM, Holmquist B, Zhao Q, Lundborg G, Kanje M (1995) Predegeneration enhances regeneration into acellular nerve grafts. Brain Res 681(1-2):105-108.
Entwistle J, Zhang S, Yang B, Wong C, Li Q, Hall CL, Jingbo A, Mowat M, Greenberg AH, Turley EA (1995) Characterization of the murine gene encoding the hyaluronan receptor RHAMM. Gene 163:233-238.
Faulk DM, Carruthers CA, Warner HJ, Kramer CR, Reing JE, Zhang L, D'Amore A, Badylak SF (2014) The effect of detergents on the basement membrane complex of a biologic scaffold material. Acta Biomater 10:183-193.
Frerichs O, Fansa H, Schicht C, Wolf G, Schneider W, Keilhoff G (2002) Reconstruction of peripheral nerves using acellular nerve grafts with implanted cultured Schwann cells. Microsurgery 22:311-315.
Geuna S, Raimondo S, Fregnan F, Haastert-Talini K, Grothe C (2016) In vitro models for peripheral nerve regeneration. Eur J Neurosci 43:287-296.
Gilbert TW, Sellaro TL, Badylak SF (2006) Decellularization of tissues and organs. Biomaterials 27:3675-3683.
Gulati AK, Cole GP (1994) Immunogenicity and regenerative potential of acellular nerve allografts to repair peripheral nerve in rats and rabbits. Acta Neurochir (Wien) 126(2-4):158-164.
Hall S (2005) The response to injury in the peripheral nervous system. J Bone Joint Surg Br 87:1309-1319.
Hudson TW, Liu SY, Schmidt CE (2004a) Engineering an improved acellular nerve graft via optimized chemical processing. Tissue Eng 10(9-10):1346-1358.
Hudson TW, Zawko S, Deister C, Lundy S, Hu CY, Lee K, Schmidt CE (2004b) Optimized acellular nerve graft is immunologically tolerated and supports regeneration. Tissue Eng 10(11-12):1641-1651.
Jia H, Wang Y, Tong XJ, Liu GB, Li Q, Zhang LX, Sun XH (2012) Sciatic nerve repair by acellular nerve xenografts implanted with BMSCs in rats xenograft combined with BMSCs. Synapse 66:256-269.
Kagami S, Kondo S, Löster K, Reutter W, Urushihara M, Kitamura A, Kobayashi S, Kuroda Y (1998) Collagen type I modulates the platelet-derived growth factor (PDGF) regulation of the growth and expression of beta1 integrins by rat mesangial cells. Biochem Biophys Res Commun 252:728-732.
Kashani IR, Zaminy A, Barbarestani M, Hedayatpour A, Mahmoudi R, Vardasbi S, Nejad AF, ali Naraghi M (2009) In vitro osteogenesis of rat adipose-derived stem cells: comparison with bone marrow stem cells. Arch Med Sci 5:149-155.
Keane TJ, Londono R, Turner NJ, Badylak SF (2012) Consequences of ineffective decellularization of biologic scaffolds on the host response. Biomaterials 33:1771-1781.
Moore AM, MacEwan M, Santosa KB, Chenard KE, Ray WZ, Hunter DA, Mackinnon SE, Johnson PJ (2011) Acellular nerve allografts in peripheral nerve regeneration: a comparative study. Muscle Nerve 44:221-234.
Osawa T, Tohyama K, Ide C (1990) Allogeneic nerve grafts in the rat, with special reference to the role of Schwann cell basal laminae in nerve regeneration. J Neurocytol 19:833-849.
Philips C, Campos F, Roosens A, Sánchez-Quevedo MDC, Declercq H, Carriel V (2018) Qualitative and quantitative evaluation of a novel detergent-based method for decellularization of peripheral nerves. Ann Biomed Eng 46:1921-1937.
Ren H, Shi X, Tao L, Xiao J, Han B, Zhang Y, Yuan X, Ding Y (2013) Evaluation of two decellularization methods in the development of a whole-organ decellularized rat liver scaffold. Liver Int 33:448-458.
Schwarzbauer J (1999) Basement membranes: Putting up the barriers. Curr Biol 9:R242-244.
Shellswell GB, Restall DJ, Duance VC, Bailey AJ (1979) Identification and differential distribution of collagen types in the central and peripheral nervous systems. FEBS Lett 106:305-308.
Siemionow M, Sonmez E (2007) Nerve allograft transplantation: a review. J Reconstr Microsurg 23:511-520.
Sondell M, Lundborg G, Kanje M (1998) Regeneration of the rat sciatic nerve into allografts made acellular through chemical extraction. Brain Res 795:44-54.
Sridharan R, Reilly RB, Buckley CT (2015) Decellularized grafts with axially aligned channels for peripheral nerve regeneration. J Mech Behav Biomed Mater 41:124-135.
Syed O, Walters NJ, Day RM, Kim HW, Knowles JC (2014) Evaluation of decellularization protocols for production of tubular small intestine submucosa scaffolds for use in oesophageal tissue engineering. Acta Biomater 10:5043-5054.
van der Rest M, Garrone R (1991) Collagen family of proteins. FASEB J 5:2814-2823.
Velardi F, Amante PR, Caniglia M, De Rossi G, Gaglini P, Isacchi G, Palma P, Procaccini E, Zinno F (2006) Osteogenesis induced by autologous bone marrow cells transplant in the pediatric skull. Childs Nerv Syst 22:1158-1166.
Wakimura Y, Wang W, Itoh S, Okazaki M, Takakuda K (2015) An experimental study to bridge a nerve gap with a decellularized allogeneic nerve. Plast Reconstr Surg 136:319-327e.
Wallis JM, Borg ZD, Daly AB, Deng B, Ballif BA, Allen GB, Jaworski DM, Weiss DJ (2012) Comparative assessment of detergent-based protocols for mouse lung de-cellularization and re-cellularization. Tissue Eng Part C Methods 18:420-432.
Walsh S, Midha R (2009) Practical considerations concerning the use of stem cells for peripheral nerve repair. Neurosurg Focus 26:E2.
Wu P, Nakamura N, Kimura T, Nam K, Fujisato T, Funamoto S, Higami T, Kishida A (2015) Decellularized porcine aortic intima-media as a potential cardiovascular biomaterial. Interact Cardiovasc Thorac Surg 21:189-194.
Xu H, Xu B, Yang Q, Li X, Ma X, Xia Q, Zhang Y, Zhang C, Wu Y, Zhang Y (2014) Comparison of decellularization protocols for preparing a decellularized porcine annulus fibrosus scaffold. PLoS One 9:e86723.
Zalewski AA, Gulati AK (1982) Evaluation of histocompatibility as a factor in the repair of nerve with a frozen nerve allograft. J Neurosurg 56:550-554.
Zilic L, Wilshaw SP, Haycock JW (2016) Decellularisation and histological characterisation of porcine peripheral nerves. Biotechnol Bioeng 113:2041-2053.
Zilic L, Garner PE, Yu T, Roman S, Haycock JW, Wilshaw SP (2015) An anatomical study of porcine peripheral nerve and its potential use in nerve tissue engineering. J Anat 227:302-314.